4. EXPERIMENTAL METHODS

In previous sections we have discussed the results of various experiments without saying anything about how such experiments are done. In this section we will take a brief look at experimental methods. The emphasis here will be on the physical principles behind the methods and not on the details.

4.1 Overview

We have already noted that to explore the structure of nuclei (nuclear physics) or hadrons (particle physics) requires projectiles whose wavelengths are at least as small as the radii of the nuclei or hadrons. This determines the minimum value of the momentum $p = h/\lambda$ and hence the energy required. Until the early 1950's the only source of high-energy particles was cosmic rays, and studies using them led to many notable discoveries. However, cosmic rays are now used only in very special circumstances, and the overwhelming majority of experiments are conducted using beams of particles produced by machines called *accelerators*. This has the great advantage that the projectiles are of a single type, and have energies that may be controlled by the experimenter. For example, beams that are essentially mono-energetic may be prepared, and can be used to study the energy dependence of interactions. The beam, once established, is directed onto a target so that interactions may be produced. In a *fixed-target* experiment the target is stationary in the laboratory. Nuclear physics experiments are invariably of this type, as are many experiments in particle physics.

In particle physics, high energies are also required to produce new and unstable particles and this reveals a disadvantage of fixed-target experiments when large centre-of-mass energies are required. The centre-of-mass energy is important because it is a measure of the energy available to create new particles. In the laboratory frame at least some of the final-state particles must be in motion to conserve momentum. Consequently, at least some of the initial beam energy must reappear as kinetic energy of final-state particles, and is unavailable for particle production. In contrast, in the centre-of-mass frame the total momentum is zero, and in principle all the energy is available for particle production.

To find the centre-of-mass energy we use the invariant (i.e. valid in all inertial frames) expression

$$E_{CM}{}^2 = \left(P_t + P_b\right)^2$$

where the subscripts t and b refer to target and beam, respectively. For a fixed-target experiment in the lab we have

$$P_t = \left(m_t c^2, \mathbf{0}\right) \; ; \qquad P_b = \left(E_L \, , \mathbf{p}_b c\right)$$

Expanding gives

$$E_{CM}{}^2 = P_t{}^2 + P_b{}^2 + 2P_t P_b$$

and using $P_t{}^2 = m_t{}^2 c^4$ etc, together with the general result

$$P_i \, P_j = E_i \, E_j - \mathbf{p}_i . \mathbf{p}_j \, c^2$$

we have

$$E_{CM} = \left[m_b{}^2 c^4 + m_t{}^2 c^4 + 2m_t c^2 E_L\right]^{1/2}$$

At high energies this increases only as $\left(E_L\right)^{1/2}$ and most of the beam energy is unavailable for particle production.

In a *colliding-beam* accelerator, two beams of particles travelling in almost opposite directions are made to collide at a small or zero crossing angle. If for simplicity we assume the particles in the two beams have the same mass and they collide at zero crossing angle with the same energy E_L, the total centre-of-mass energy is

$$E_{CM} = 2E_L$$

This increases linearly with the energy of the accelerated particles, and is hence a significant improvement on the fixed-target result. Colliding beam experiments are not however without their own disadvantages. The colliding particles have to be stable, which limits the interactions that can be studied, and the collision rate in the intersection region is generally smaller than that achieved in fixed-target experiments, because the beam densities are low compared to a solid or liquid target.

Finally, details of the particles produced in the collision (e.g. their momenta) are deduced by observing their interactions with the material of *detectors*, which are placed in the vicinity of the interaction region. A wide range of detectors is available, each with specific characteristics, and modern experiments, particularly in particle physics, typically use several types in a single experiment.

In this section we start by briefly describing some of the different types of accelerator that have been built, and the beams that they can produce. Then we discuss the ways in which particles interact with matter, and review how these mechanisms are exploited in the construction of a range of particle detectors.

4.2 Accelerators

All accelerators use electromagnetic forces to boost the energy of stable charged particles. These are injected into the machine from a device that provides a high intensity source of low energy particles, for example an electron gun (a hot filament), or a proton ion source.

The accelerators used for nuclear structure studies may be classified in to those that develop a steady accelerating field and those in which radio frequency electric fields are used. All accelerators for particle physics are of the latter type. The most important example of the former type is the Van de Graaff accelerator, which is shown schematically in Fig.4.1. The key to this type of device is to establish a very high voltage. The Van de Graaff accelerator achieves this by using the fact that the charge on a conductor resides on its outermost surface and hence if a conductor carrying charge touches another conductor it will transfer its charge to the outer conductor. In Fig.4.1, positive ions produced at P are sprayed onto a belt at S, which passes over motor-driven pulleys R. At C there is a collector, which collects the charges, which are then transferred to the outer surface of a large metal sphere. In this way a high voltage is established and ions from a source can be accelerated down a vacuum tube onto a target. This account ignores many technical details. For example, the dome is filled with an inert gas at high pressure to minimise electrical breakdown by the high voltage. A simple Van de Graaff accelerator can achieve a potential of about 12 MeV and a modification called a tandem Van de Graaff can effectively double this.

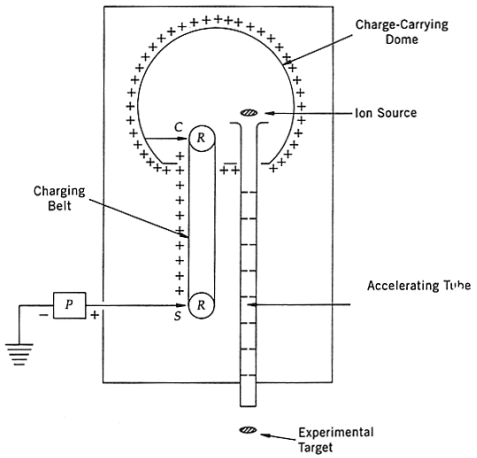

Fig.4.1 The principle of the Van de Graaff accelerator

Accelerators using radio frequency electric fields may conveniently be divided into *linear* and *cyclic* varieties. In a linear accelerator (or *linac*) for acclerating ions, bunches of particles pass through a series of metal tubes called *drift tubes*, that are located in a vacuum vessel and connected successively to alternate terminals of a radio frequency oscillator, as shown in Fig.4.2.

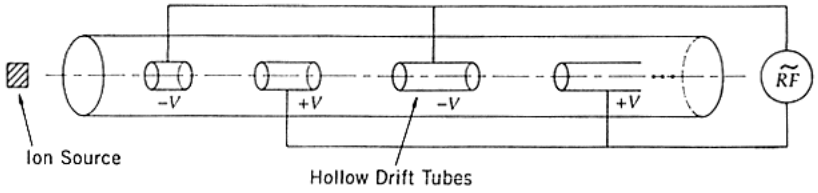

Fig.4.2 Acceleration in a linear accelerator

Positive ions are accelerated by the field towards the first drift tube. If the alternator can change its direction before the ion passes through that tube, then they will be accelerated again on their way between the exit of the first and entry to the second tube, and so on. Because the particles are accelerating, the lengths of the drift tubes has to increase to ensure continuous acceleration. Electrons are accelerated by a variation of this method. In this case, bunches of particles pass through a straight evacuated waveguide with a periodic array of gaps, similar to the ion accelerator. Radio frequency oscillations in the gaps are used to establish a moving electromagnetic wave in the structure, with a longitudinal component of the electric field moving in phase with the particles. As long as this phase relationship can be maintained, the particles will be continuously accelerated.

Cyclic accelerator used for low-energy nuclear physics experiments are of a type called *cyclotrons;* they operate in a somewhat different way to those used in particle physics, which

are called *synchrotrons*. We will describe the operation of just the latter. In a synchrotron, the beam of particles travels in a vacuum pipe called the *beam pipe* and is constrained in a circular or near circular path by an array of dipole magnets called bending magnets. (See Fig.4.3a.) Acceleration is achieved as the beam repeatedly traverses one or more cavities placed in the ring. Since the particles travel in a circular orbit they continuously emit radiation, called in this context *synchrotron radiation*. The amount of energy radiated per turn by a relativistic particle of mass m is proportional to $1/m^4$. For electrons the losses are thus very severe, and the need to compensate for these by the input of large amounts of rf power limits the energies of electron synchrotrons.

The momentum in GeV/c of an orbiting particle assumed to have unit charge is given by $p = 0.3B\rho$, where B is the magnetic field in Tesla and ρ, the radius of curvature, is measured in metres. Because p is increased during acceleration, B must also be steadily increased if ρ is to remain constant, and the final momentum is limited both by the maximum field available and by the size of the ring. With conventional electromagnets, the largest field attainable over an adequate region is about 1.5T, and even with superconducting coils it is only of order 5T. Hence the radius of the ring must be very large to achieve very high energies. For example the Tevatron accelerator has a radius of l km. A large radius is also important to limit synchrotron radiation losses in electron machines.

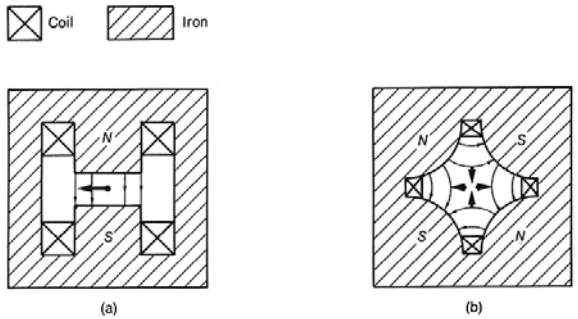

Fig.4.3 Cross-section of (a) typical bending (dipole) magnet and (b) focusing quadrupole) magnet. The light arrows indicate field directions; the heavy arrows, the force on a positive particle travelling into the paper.

In the course of its acceleration, a beam may make typically 10^5 traversals of its orbit before reaching its maximum energy. Consequently stability of the orbit is vital, both to ensure that the particles continue to be accelerated, and that they do not strike the sides of the vacuum tube. In practice the particles are accelerated in bunches, each being synchronised with the rf field. In equilibrium a particle increases its momentum just enough to keep the radius of curvature constant as the field B is increased during one rotation, and the circulation frequency of the particle is “in step” with the rf of the field. In practice, the particles remain in the bunch, but their trajectories oscillate about the stable orbits. These oscillations are controlled by a series of focussing magnets, usually of the quadrupole type, which are placed at intervals around the beam and act like optical lenses. A schematic diagram of one of these is shown in Fig.4.3b. Each focuses the beam in one direction and so alternative magnets have their field directions reversed.

In addition to the energy of the beam, one is also concerned to produce a beam of high intensity, so that interactions will be plentiful. The intensity is ultimately limited by defocussing effects, e.g. the mutual repulsion of the particles in the beam, and a number of technical problems have to be overcome which are outside the scope of this brief account.

Both linear and cyclic accelerators can be divided into *fixed-target* and *colliding beam* machines. The latter are also known as *colliders*, or in the case of cyclic machines, *storage rings*. In fixed-target machines, particles are accelerated to the highest operating energy and then the beam is extracted from the machine and directed onto a stationary target, which is usually a solid or liquid. Much higher energies have been achieved for protons than electrons, because of the large radiation losses inherent in electron machines mentioned earlier. The intensity of the beam is such that large numbers of interactions can be produced, which can either be studied in their own right or used to produce secondary beams.

The performance of a collider is characterized by the luminosity, which was defined in Section 1. The general formula given there reduces in this case to

$$L = n\frac{N_1 N_2}{A} f$$

where $N_i (i = 1,2)$ are the numbers of particles in the n colliding bunches, A is the cross-sectional area of the beam and f is the frequency, i.e. $f = 1/T$, where T is the time taken for the particles to make one traversal of the ring.

4.3 Beams

While the accelerated (primary) beams are restricted to stable charged particles, secondary beams can be neutral and/or unstable. These are considerable advantages, and historically much of our detailed knowledge of particle physics has been derived from fixed-target experiments. The main disadvantage of fixed-target machines has been mentioned earlier: the need to achieve large centre-of-mass energies to produce new particles. Most new machines are therefore colliders.

The particles which are used in accelerators must be stable and charged. One is also interested in the interaction of neutral particles, e.g. photons, as well as those of unstable particles (such as the charged pions mentioned earlier). Beams appropriate for performing such experiments can be formed provided only that they live long enough to travel appreciable distances in the laboratory. This is done by directing an extracted primary beam onto a heavy target. In the resulting interactions with the target nuclei, many new particles are produced which are then analysed into secondary beams of well-defined momentum. Such beams will ideally consist predominantly of particles of one type, but if this cannot be achieved then the wanted species may have to be identified by other means. In addition, if these secondary beams are composed of unstable particles, they can themselves be used to produce further beams formed from their decay products.

Two examples will illustrate how in principle secondary beams can be formed. Consider firstly the construction of a π^+ beam from a primary beam of protons. By allowing the protons to interact with a heavy target, secondary particles, which are mostly pions, will be produced. A collimator can then be used to select particles in a particular direction, and the π^+ component can subsequently be removed and focussed into a mono-energetic beam by selective use of electrostatic fields and bending and focussing magnets. The π^+ is itself unstable and, as we have seen, decays via the weak interaction with a lifetime of about 10^{-6}s,

primarily to a muon and a mu-neutrino, i.e. $\pi^+ \to \mu^+ + \nu_\mu$. So if the pions are passed down a long vacuum pipe, many will decay in flight to give muons and neutrinos, which will mostly travel in essentially the same direction as the initial beam. The muons and any remaining pions can then be removed by passing the beam through a very long absorber, leaving the neutrinos. In this case the final beam will have a momentum spectrum reflecting the initial momentum spectrum of the pions, and since neutrinos are neutral, no further momentum selection using magnets is possible.

4.4 Particle interactions with matter

In order to be detected, a particle must undergo an interaction with the material of a detector. In this section we discuss these interactions, but only in sufficient detail to be able to understand the detectors themselves.

The first possibility is that the particle interacts with an atomic nucleus. For example, this could be via the strong nuclear interaction if it is a hadron, or by the weak interaction if it is a neutrino. Both are *short-range interactions*. If the energy is sufficiently high, new particles may be produced, and such reactions are often the first step in the detection process. In addition to these short-range interactions, a charged particle will also excite and ionise atoms along its path, giving rise to *ionization energy losses*, and emit radiation, leading to *radiation energy losses*. Both of these processes are due to the long-range electromagnetic interaction. They are important because they form the basis of many detectors for charged particles. Photons are also directly detected by electromagnetic interactions, and at high energies their interactions with matter lead predominantly to the production of e^+e^- pairs via the process $\gamma \to e^+ + e^-$ (*pair production*), which has to occur in the vicinity of a nucleus to conserve energy and momentum.

(a) Short-range interactions with nuclei

For hadrons, the most important short-range interactions with nuclei are due to the strong nuclear force which, unlike the electromagnetic interaction, is as important for neutral particles as for charged ones. Both *elastic scattering* and *inelastic reactions* may result. At high energies, many inelastic reactions are possible, most of them involving the production of several particles in the final state. The total cross-section σ_{tot}, which we have met before, is the sum of the elastic σ_{el} and inelastic σ_{inel} cross-sections.

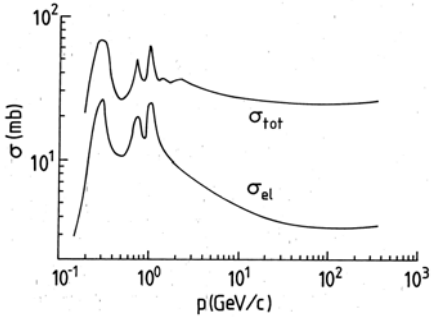

Fig.4.4 Total and elastic cross-sections for $\pi^- p$ scattering as a function of the pion laboratory momentum

Many hadronic cross-sections show considerable structure at low energies due to the production of hadronic resonances (which we have discussed briefly in Section 3), but at energies above about 3GeV total cross-sections are usually slowly varying in the range $10-50\,\text{mb}$ and are much larger than the elastic cross-section. (An example is shown in Fig.4.4.) This is of the same order-of-magnitude as the "geometrical" cross-section $\pi r^2 \approx 30\,\text{mb}$, where $r \approx 1\,\text{fm}$ is the approximate range of the strong interaction between hadrons. Total cross-sections on nuclei are much larger, increasing *roughly* like the square of the nuclear radius.

The probability of a hadron-nucleus interaction occurring as the hadron traverses a small thickness dx of material is given by $n\sigma_{tot}\,dx$, where n is the number of nuclei per unit volume in the material. Consequently, the mean distance traveled before an interaction occurs is given by

$$\ell_c = 1/n\sigma_{tot}$$

This is called the *collision length*. An analogous quantity is the *absorption length*, defined by

$$\ell_a = 1/n\sigma_{inel}$$

which governs the probability of an inelastic collision. In practice, $\ell_c \approx \ell_a$ at high energies. As examples, the interaction lengths are between 10 and 40 cm for nucleons of energy in the range 100-300 GeV interacting with metals such as iron.

Neutrinos and antineutrinos can also be absorbed by nuclei, leading to reactions of the type

$$\overline{\nu}_\ell + p \to \ell^+ + X$$

where ℓ is a lepton and X denotes any hadron or set of hadrons allowed by the conservation laws. Such processes are of course weak interactions (because they involve neutrinos) and the associated cross-sections are extremely small compared to the cross-sections for strong interaction processes. The corresponding interaction lengths are therefore enormous. Nonetheless, in the absence of other possibilities such reactions are the basis for detecting neutrinos. Finally, photons can be absorbed by nuclei, giving *photoproduction* reactions such as $\gamma + p \to X$. However, these electromagnetic interactions are not normally used to detect photons, because they occur much less readily than e^+e^- pair production in the Coulomb field of the nucleus.

(b) Ionization energy losses

Ionization energy losses are important for all charged particles, and for particles other than electrons and positrons they dominate over radiation energy losses at all but the highest attainable energies. The theory of such losses, which are due dominantly to Coulomb scattering from the atomic electrons, was worked out by Bethe, Bloch and others in the 1930's. The result is called the Bethe-Bloch formula, and for spin-0 bosons with charge $\pm q$ (in units of e), mass M and velocity v, takes the form

$$-\frac{dE}{dx} = \frac{Dq^2 n_e}{\beta^2}\left[\ell n\left(\frac{2m_e c^2\beta^2\gamma^2}{I}\right) - \beta^2 - \frac{\delta(\gamma)}{2}\right]$$

where x is the distance travelled through the medium;

$$D = \frac{4\pi\alpha^2\hbar^2}{m_e} = 5.1\text{x}10^{-25}\,\text{MeV cm}^2$$

m_e is the electron mass, $\beta = v/c$ and $\gamma = E/Mc^2 = (1-\beta^2)^{-1/2}$. The other constants refer to the properties of the medium: n_e is the electron density; I is the mean ionization potential of the atoms averaged over all electrons, which is given approximately by $I = 10Z\,\text{eV}$ for Z greater than 20; and $\delta(\gamma)$ is a dielectric screening correction, which is important only for highly relativistic particles. The corresponding formula for spin-1/2 particles differs from this, but in practice the differences are small and may be neglected in discussing the main features of ionization energy loses.

A typical example of the behaviour of $-dE/dx$ for pions and protons traversing a solid is shown in Fig.4.5. As can be seen, $-dE/dx$ falls rapidly as the velocity increases from zero because of the $1/\beta^2$ factor in the Bethe-Bloch equation. All particles have a region of "minimum ionization" for $\beta\gamma$ in the range 3 to 4. Beyond this, β tends to unity, and the logarithmic factor in the Bethe-Bloch formula gives a "relativistic rise" in $-dE/dx$, which eventually slows down as the screening correction δ becomes important. The magnitude of the energy loss depends on the medium. The electron density is given by

$$n_e = \rho NZ/A$$

where N is Avogadro's number, and ρ and A are the mass density and atomic weight of the medium, so the mean energy loss is proportional to the density of the medium. The remaining dependence on the medium is relatively weak because $Z/A \approx 0.5$ for all atoms except hydrogen and the very heavy elements, and because the ionization energy I only enters the Bethe-Bloch formula logarithmically. Ionization losses are proportional to the squared charge of the particle, so that a fractionally charged quark with $\beta\gamma \geq 3$ would have a much lower rate of energy loss than the minimum energy loss of any integrally charged particle. This has been used as a means of identifying possible free quarks, but without success.

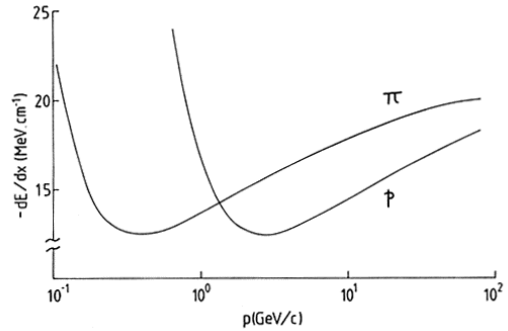

Fig.4.5 Ionization energy loss for charged pions and protons in lead

(c) Radiation energy losses

When a charged particle traverses matter it can also lose energy by radiative collisions, especially with nuclei. The electric field of a nucleus will accelerate and decelerate the particles as they pass, causing them to radiate photons, and hence lose energy. This process is called *bremsstrahlung* (literally "braking radiation" in German) and is a particularly important contribution to the energy loss for electrons and positrons.

The dominant Feynman diagrams for electron bremsstrahlung in the field of a nucleus

$$e^- + (Z,A) \rightarrow e^- + \gamma + (Z,A)$$

are shown in Fig.4.6 and are of order $Z^2\alpha^3$. The presence of the nucleus is to absorb the recoil energy and so ensure that energy and momentum are simultaneously conserved. (Recall the original discussion of Feynman diagrams.)

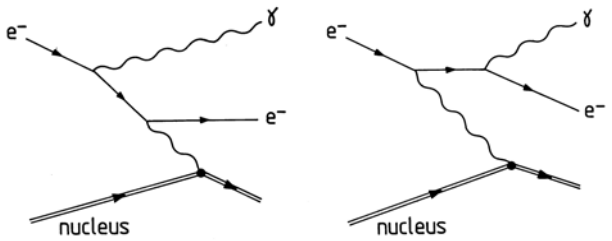

Fig.4.6 Dominant Feynman diagrams for the bremsstrahlung process

$$e^- + (Z,A) \rightarrow e^- + \gamma + (Z,A)$$

There are also contributions from bremsstrahlung in the fields of the atomic electrons, each of order α^3. Since there are Z atomic electrons for each nucleus, these give a total contribution of order $Z\alpha^3$, which is small compared to the contribution from the nucleus for all but the lightest elements. A detailed calculation shows that for relativistic electrons with $E \gg mc^2/\alpha Z^{1/3}$, the average rate of energy loss is given by

$$-\frac{dE}{dx} = \frac{E}{L_R}$$

The constant L_R is called the *radiation length* and is a function of Z and n_a, the density of atoms/cm^3 in the medium. It follows that the radiation length is the average thickness of material that reduces the mean energy of an electron or positron by a factor e. For example, the radiation length in lead is about 2 cm.

From these results, we see that at high energies the radiation losses are proportional to E/m^2, or more generally E/m_P^2 for an arbitrary charged particle of mass m_p. On the other hand, the ionization energy losses are only weakly dependent on the projectile mass and energy at very high energies. Consequently, radiation losses completely dominate the energy losses for electrons and positrons at high enough energies, but are much smaller than

ionization losses for all particles other than electrons and positrons at all but the highest energies.

(d) Interactions of photons in matter

In contrast to heavy charged particles, photons have a high probability of being absorbed or scattered through large angles by the atoms in matter. Consequently, a collimated monoenergetic beam of I photons per second traversing a thickness dx of matter will lose

$$dI = -I\frac{dx}{\lambda}$$

photons per second, where

$$\lambda = (n_a\sigma_\gamma)^{-1}$$

is the mean free path before absorption or scattering out of the beam, and σ_γ is the total photon interaction cross-section with an atom. The mean free path λ is analogous to the collision length for hadronic reactions. Integrating the above equation gives

$$I(x) = I_0\, e^{-x/\lambda}$$

for the intensity of the beam as a function of distance, where I_0 is the initial intensity.

The main processes contributing to σ_γ are the *photoelectric effect*, in which the photon is absorbed by the atom as a whole with the emission of an electron; the *Compton effect*, where the photon scatters from an atomic electron; and *electron-positron pair production* in the field of a nucleus or of an atomic electron. The corresponding cross-sections on lead are shown in Fig.4.7.

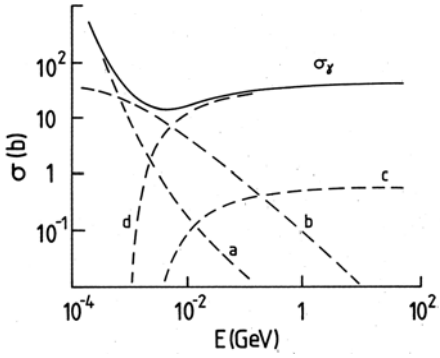

Fig.4.7 Total photon cross-section σ_γ on a lead atom, together with the contributions from (a) the photoelectric effect, (b) Compton scattering, (c) pair production in the field of the atomic electrons, and (d) pair production in the field of the nucleus.

The pair production process is closely related to electron bremsstrahlung, as can be seen by comparing the Feynman diagrams shown in Figs.4.6 and 4.8. The cross-section for pair production rises rapidly from threshold, and is given to a good approximation by

$$\sigma_{pair} = \frac{7}{9}\frac{1}{n_a L_R}$$

for $E_\gamma \gg mc^2/\alpha Z^{1/3}$, where L_R is the radiation length. Substituting these results into the expression for $I(x)$, gives

$$I(x) = I_0 \exp(-7x/9L_R)$$

so that at high energies photon absorption, like electron radiation loss, is characterised by the radiation length L_R.

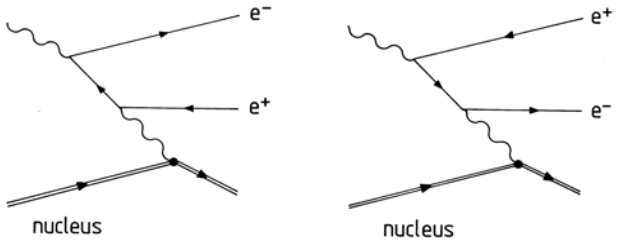

Fig.4.8 The pair production process $\gamma + (Z,A) \rightarrow e^- + e^+ + (Z,A)$

4.5 Particle detectors

The detection of a particle means more than simply its localization. To be useful this must be done with a resolution sufficient to enable particles to be separated in both space and time in order to determine which are associated with a particular event. We also need to be able to identify each particle and measure its energy and momentum. No single detector is optimal with respect to all these requirements. Many of the devices discussed below are commonly used both in nuclear and particle physics, but in the former a single type of detector is often sufficient, whereas in particle physics, both at fixed-target machines and colliders, the modern trend is to build very large multi-component detectors which integrate many different sub-detectors in a single device. Such systems rely heavily on fast electronics and computers to monitor and control the sub-detectors, and to co-ordinate, classify, and record the vast amount of information flowing in from different parts of the apparatus. In this section we will briefly introduce some of the most important detectors currently available.

(a) Time resolution: scintillation counters

For charged particles we have seen that energy losses occur due to excitation and ionization of atomic electrons in the medium of the detector. In suitable materials, called "scintillators", a small fraction of the excitation energy re-emerges as visible light during de-excitation. In a *scintillation counter* this light passes down the scintillator and is directed onto the face of a photomultiplier (a device which converts a weak photon signal to a detectable electric impulse) by multiple internal reflections along a shaped solid plastic tube called a light guide, and the whole assembly is made light-tight to prevent background light reaching the photomultiplier tube. A schematic diagram of a photomultiplier tube is shown in Fig.4.9.

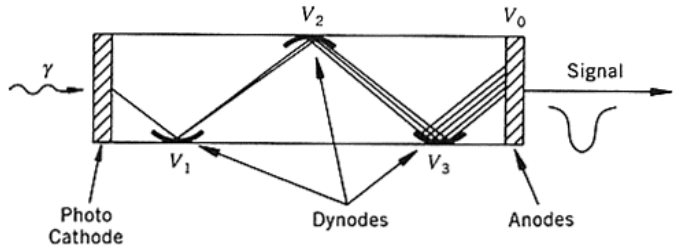

Fig.4.9 Schematic diagram of the main elements of a photomultiplier tube

Electrons are emitted from the cathode of the photomultiplier by the photoelectric effect and strike a series of focussing dynodes. These amplify the electrons by secondary emission at each dynode and accelerate the particles to the next stage. The final signal is extracted from the anode at the end of the tube. The electronic pulse can be as short as 10 ns because of the very short decay time of the scintillator. The scintillation counter is thus an ideal timing device and it is widely used for "triggering" other detectors, i.e. its signal is used to decide whether or not to activate other apparatus, and whether to record information from the event. Commonly used scintillators are inorganic single crystals (e.g. sodium iodide) or organic liquids and plastics, and a modern complex detector may use several tons of detector in combination with thousands of photomultiplier tubes. (The Super Kamiokande experiment mentioned in Section 2, which detected neutrino oscillations, has 11,000 such tubes.) The robust and simple nature of the scintillation counter has made it a mainstay of experimental particle physics since the earliest days of the subject.

(b) Measurement of position

There is a wide range of devices available that provide accurate measurements of a particle's position. All these devices detect ionization, either by collecting the total ionization products onto electrodes using an electric field, or by making the ionization track visible in some form. Historically important examples of the latter are stacks of photographic emulsions, cloud chambers, and bubble chambers, but none of these are now in general use and all have been replaced by electronic detectors.

<u>Proportional and drift chamber</u>

The basis of proportional chambers, and of other gaseous detectors, is the observation that if an electric field is established in a gas, then the electrons released as part of electron-ion pairs by the passage of a charged particle will drift towards the anode. If the field is strong enough, an electron will gain sufficient energy to cause secondary ionization, and a chain of such processes leads to an avalanche of secondary electrons which can be collected as a pulse on the anode. In practice the gas mixture must contain at lease one "quenching" component which absorbs ultraviolet light and stops the plasma spreading throughout the gas. For electric fields of order $10^4 - 10^5$ V/cm, the number of secondary electrons is proportional to the number of primary ion pairs, and is typically 10^5 per primary ion pair.

The earliest detector using this idea was the *proportional counter*, which consists basically of a cylindrical tube filled with gas and maintained at a negative potential, and a fine central anode wire at a positive potential. Subsequently, the resolution of proportional counters was greatly improved as a result of the discovery that if many anode wires were arranged in a plane between a common pair of cathode plates, each wire acts as an independent detector.

This device is called a *multiwire proportional chamber* (MWPC), and has been a major ingredient in detector systems since its introduction in 1968. A MWPC can achieve spatial resolutions of 500 μm or less, and has a typical time resolution of about 30 ns. A schematic diagram of a MWPC is shown in Fig.4.10.

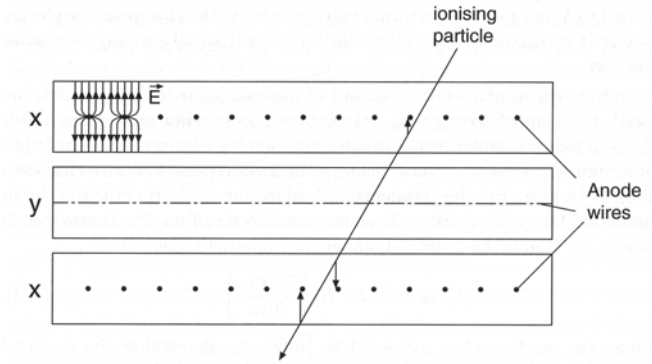

Fig.4.10 A group of three proportional chambers. The anode wires of the x-layers point into the page; those of the y-layers run at right angles. The cathodes are the edges of the chambers. A positive voltage applied to the anode wires generates a field as shown in the upper corner. A particle crossing the chamber ionizes the gas and the electrons drift along the field lines to the anode wires. In this example, there would signals from one wire in the upper x-plane and two in the lower x-plane.

MWPC's with high resolution are expensive because of the need to read out signals from a very large number of wires. This cost can be reduced significantly, and even better spatial resolutions obtained, in a device called a *drift chamber*, which has now largely replaced the MWPC as a general detector. This uses the fact that the liberated electrons take time to drift from their point of production to the anode. Thus the time delay between the passage of a charged particle through the chamber and the creation of a pulse at the anode is related to the distance between the particle trajectory and the anode wire. In practice, a reference time has to be defined, which for example could be done by allowing the particle to pass through a scintillator positioned elsewhere in the experiment. The electrons drift for a time and are then collected at the anode, thus providing a signal that the particle has passed. If the drift time can be measured accurately (to within a few ns) and if the drift velocity is known, then spatial resolutions of 100-200 μm can easily be achieved, and specialised detectors can reduce this still further.

Multiwire proportional chambers and drift chambers are both constructed in a variety of geometries to suit the nature of the experiment, and arrangements where the wires are in planar, radial, or cylindrical configurations have all been used. The latter type are also called "jet chambers" and the two-jet event I showed in an earlier lecture as evidence for the existence of quarks (Fig.3.3) was obtained using a jet chamber.

Semiconductor detectors

Semiconductor detectors are essentially solid state ionization chambers with the electron-hole pairs ('holes' are the 'absence' of electrons and act like positrons) playing the role of electron-ion pairs in gas detectors. In the presence of an electric field, the electrons and holes separate and collect at the electrodes, giving a signal proportional to the energy loss of the

incident charged particle. Such detectors have long been used in nuclear physics, but have only more recently become important in particle physics, because they are small and cannot be used to cover large areas at reasonable cost. For example, in a silicon microstrip detector, narrow strips of active detector are etched onto a thin slice of silicon, with gaps of order l0μm, to give a tiny analogue of a MWPC. Arrays of such strips can then be used to form detectors with resolutions of order 5μm, which can, for example, be placed close to the interaction vertex in a colliding beam experiment, with a view to studying events involving the decay of very short-lived particles. Such solid state "vertex detectors" are becoming increasingly important in particle physics and have been incorporated in several of the multi-component detectors designed for use in the new generation of colliders. Their main advantage is their superb spatial resolution; their main disadvantage is their limited ability to withstand radiation damage.

(c) Measurement of momentum

The momentum of a charged particle is usually determined from the curvature of its track in an applied magnetic field. It is common practice to enclose track chambers in a magnetic field to perform momentum analysis. An apparatus, which is dedicated to measuring momentum, is called a *spectrometer*. It consists of a magnet and a series of detectors to track the passage of the particles. The precise design depends on the nature of the experiment being undertaken. For example, in a fixed-target experiment at high energies, the reaction products are usually concentrated in a narrow cone about the initial beam direction, whereas in colliding beam experiments spectrometers must completely surround the interaction region to obtain full angular coverage.

Magnet designs vary. Dipole magnets typically have their field perpendicular to the beam direction. They have their best momentum resolution for particles emitted forward and backward with respect to the beam direction, and are often used in fixed-target experiments at high energies. However, the beam will be deflected, and so at colliders this must be compensated for elsewhere to keep the particles in orbit. At colliders the most usual magnet shape is the solenoid where the field lines are essentially parallel to the beam direction. This device is used in conjunction with cylindrical tracking detectors, like jet chambers, and has its best momentum resolution for particles perpendicular to the beam direction.

(d) Particle identification

Methods of identification are usually based on determining the mass of the particle by simultaneous measurements of its momentum together with some other quantity. At low $\gamma = E/mc^2$ values, measurements of the rate of energy loss dE/dx can be used, while muons may be characterised by their unique penetrating power in matter, as we have already seen. Here we concentrate on methods based on measuring the velocity or energy, assuming always that the momentum is known (from a spectrometer, for example).

Time-of-flight

The simplest method, in principle, is to measure the time of flight between, for example, two scintillation counters. This is used, for example, in experiments using low-energy neutron beams. However, since all high-energy particles have velocities close to the speed of light, this method is usually limited to particles with momenta less than about 4 GeV/c.

Čerenkov counters

The most important identification method for high-energy particles is based on the Čerenkov effect. When a charged particle with velocity v traverses a dispersive medium of refractive

index n, excited atoms in the vicinity of the particle become polarized, and if v is greater than the speed of light in the medium c/n, a part of the excitation energy reappears as coherent radiation emitted at a characteristic angle θ to the direction of motion. The necessary condition $v > c/n$ implies

$$\beta n > 1$$

and by considering how the waveform is produced (this is called Huygen's construction in optics) it can be shown that

$$\cos\theta = 1/\beta n$$

for the angle θ, where $\beta = v/c$ as usual. A determination of θ is thus a direct measurement of the velocity.

Čerenkov radiation appears as a continuous spectrum and may be collected onto a photosensitive detector. Its main limitation from the point of view of particle detection is that so few photons are produced. In general, the number of photons $N(\lambda)d\lambda$ radiated per unit path length in a wavelength interval $d\lambda$ can be shown to be

$$N(\lambda)\,d\lambda = 2\pi\alpha\left(1-\frac{1}{\beta^2 n^2}\right)\frac{d\lambda}{\lambda^2} \;<\; 2\pi\alpha\left(1-\frac{1}{n^2}\right)\frac{d\lambda}{\lambda^2}$$

and vanishes rapidly as the refractive index approaches unity. The maximum value occurs for $\beta = 1$, and, for example, for a particle with unit charge, corresponds to about 200 photons/cm in the visible region in water and glass. These numbers should be compared to the 10^4 photons/cm emitted in a typical scintillator. Because they are so small, appreciable lengths are needed to give enough photons, and gas Čerenkov counters in particular can be several metres long.

Čerenkov counters are used in two different modes. The first is as a *threshold counter* to detect the presence of particles whose velocities exceed some minimum value. Suppose that two particles with β values β_1 and β_2 at some given momentum p are to be distinguished. If a medium can be found such that $\beta_1 n > 1 \geq \beta_2 n$, then particle 1 will produce Čerenkov radiation but particle 2 will not. Clearly, to distinguish between highly relativistic particles with $\gamma \gg 1$ also requires $n \approx 1$, so that from the equation above very few photons are produced. Nevertheless, common charged particles can be distinguished in this way up to at least 30 GeV/c.

Another device is the so-called *ring-image* Čerenkov detector and is a very important device at both fixed-target machines and colliders. If we assume that the particles are not all travelling parallel to a fixed axis, then the radiating medium can be contained within two concentric spherical surfaces of radii R and 2R centred on the target or interaction region where the particles are produced, as illustrated in Fig.4.11. The outer surface is lined with a mirror, which focuses the Čerenkov radiation into a ring at the inner detector surface. The radius of this ring depends on the angle θ at which the Čerenkov radiation is emitted, and hence on the particle velocity v. It is determined by constructing an image of the ring electronically.

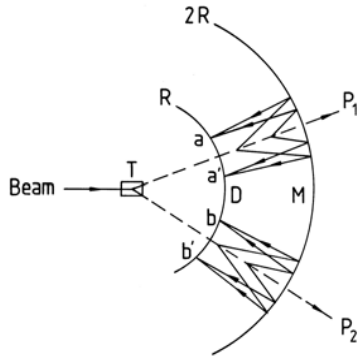

Fig.4.11 Two particles P_1 and P_2, emitted from the target T, emit Čerenkov radiation on traversing a medium contained between two spheres of radius R and 2R. The mirror M on the outer sphere focuses the radiation into ring images at aa′ and bb′ on the inner detector sphere D. The radii of the ring images depend on the angle of emission of the Čerenkov radiation and hence on the velocities of the particles.

Transition radiation

In the ultra high-energy region ($\gamma \geq 1000$) methods which are sensitive to a particle's velocity are not very useful. However, in this regime a direct measurement of γ is possible by detecting *transition radiation.* This occurs whenever charged particles traverse the interface between substances with different dielectric properties. Its importance stems from the fact that the intensity of the emitted radiation (which is in the X-ray region) is sensitive to the particle's energy $E = mc^2\gamma$ rather than its velocity. Transition radiation is particularly useful for the "non-destructive" identification of electrons.

(e) Energy measurements: calorimeters

Calorimeters are an important class of detector used for measuring the energy and position of a particle by its total absorption and are widely used in particle physics experiments. They differ from most other detectors in that the nature of the particle is changed by the detector, and in that they can detect neutral as well as charged particles. A calorimeter may be a homogeneous absorber/detector, such as a block of lead glass used to detect photons by Čerenkov radiation emitted by e^+e^- pairs created in the Coulomb fields of the nuclei. Alternatively, it can be a sandwich construction with separate layers of absorber (e.g. a metal such as lead) and detector (scintillator, MWPC etc). The latter are also known as "sampling calorimeters". During the absorption process, the particle will interact with the material of the absorber, generating secondary particles which will themselves generate further particles and so on, so that a cascade or shower, develops. For this reason calorimeters are also called "shower counters".

The shower is predominantly in the longitudinal direction, but will be subject to some transverse spreading due both to multiple Coulomb scattering and the transverse momentum of the produced particles. Eventually all, or almost all, of the primary energy is deposited in the calorimeter, and gives a signal in the detector part of the device. A schematic diagram of a calorimeter for detection of the energy of an electromagnetic shower is shown in Fig.4.12.

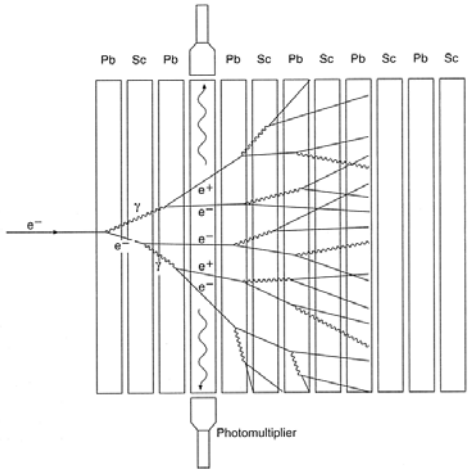

Fig.4.12 Electromagnetic shower development inside a sampling calorimeter. (The particle tracks are not continued to the rear of the detector.)

There are several reasons why calorimeters are important, especially at high energies; (i) they can detect neutral particles, by detecting the charged secondaries; (ii) the absorption process is statistical, so that the relative precision of energy measurements $\Delta E/E$ varies like $E^{-1/2}$ for large E, which is a great improvement on high-energy spectrometers where $\Delta E/E$ varies like E^2 ; and (iii) the signal produced can be very fast, of order (10-100)ns, and is ideal for making triggering decisions.

Although it is possible to build calorimeters that preferentially detect just one class of particle (electrons and photons, or hadrons) it is also possible to design detectors which serve both purposes. Since the characteristics of electromagnetic and hadronic showers are somewhat different it is convenient to describe each separately.

Electromagnetic showers

When a high-energy electron or positron interacts with matter we have seen that the dominant energy loss is due to bremsstrahlung, and for the photons produced the dominant absorption process is pair production. Thus the initial electron will, via these two processes, lead to a cascade of $e^{\pm}$ pairs and photons, and this will continue until the energies of the secondary electrons fall below the critical energy E_C where ionization losses equal those from bremsstrahlung. This energy is roughly given by $E_C \approx 600\,\mathrm{MeV}/Z$.

Most of the correct qualitative features of shower development may be obtained from the following simple model. We assume: (i) each electron with $E > E_C$ travels one radiation length and then gives up half of its energy to a bremsstrahlung photon; (ii) each photon with $E > E_C$ travels one radiation length and then creates an electron-positron pair with each particle having half the energy of the photon; (iii) electrons with $E < E_C$ cease to radiate and lose the rest of their energy by collisions; (iv) ionization losses are negligible for $E > E_C$. The development of the shower in this model is shown in Fig.4.13.

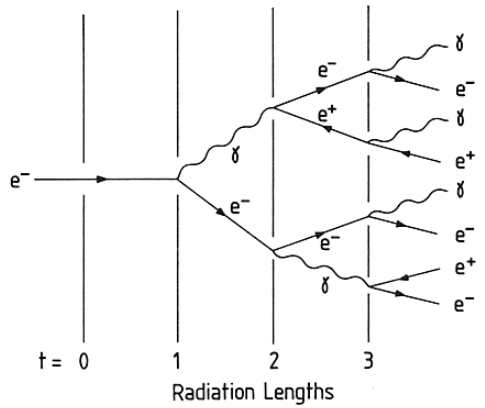

Fig.4.13 Simple model for the development of an electromagnetic shower

If the initial electron has energy $E_0 \gg E_C$, then after t radiation lengths the shower will contain 2^t particles, which consist of approximately equal numbers of electrons, positrons and photons each with an average energy

$$E(t) = E_0 / 2^t \quad .$$

The shower will cease abruptly when $E(t) = E_C$, i.e. at $t = t_{\max}$ where

$$t_{\max} = t(E_C) \equiv \frac{\ell n(E_0/E_C)}{\ell n 2}$$

and the number of particles at this point will be

$$N_{\max} = \exp[t_{\max}\,\ell n 2] = E_0/E_C$$

The main features of this simple model are observed experimentally, and in particular the maximum shower depth increases only logarithmically with primary energy. Because of this, the physical sizes of calorimeters need increase only slowly with the maximum energies of the particles to be detected. The energy resolution of a calorimeter, however, depends on statistical fluctuations, which are neglected in this simple model, but for an electromagnetic calorimeter it is typically $\Delta E / E \approx 0.05 / \sqrt{E}$, where E is measured in GeV.

Hadronic showers

Although hadronic showers are qualitatively similar to electromagnetic ones, shower development is far more complex because many different processes contribute to the inelastic production of secondary hadrons. The scale of the shower is determined by the nuclear absorption length defined earlier. Since this absorption length is larger than the radiation length, which controls the scale of electromagnetic showers, hadron calorimeters are thicker devices than electromagnetic ones. Another difference is that some of the contributions to the total absorption may not give rise to an observable signal in the detector. Examples are

nuclear excitation and leakage of secondary muons and neutrinos from the calorimeter, and the loss of "visible" or measured energy for hadrons is typically 20-30% greater than that for electrons.

The energy resolution of calorimeters is in general much worse for hadrons than for electrons and photons because of the greater fluctuations in the development of the hadron shower. Depending on the proportion of π^0's produced in the early stages of the cascade, the shower may develop predominantly as an electromagnetic one because of the decay $\pi^0 \rightarrow \gamma\gamma$. These various features lead to an energy resolution typically about a factor of 5-10 poorer than for electromagnetic calorimeters.

4.6 Layered detectors

As stated earlier, in particle physics it is necessary to combine several detectors in a single experiment to extract the maximum amount of information from it. Typically, working out from the interaction region, there will be a series of wire chambers, followed further out by calorimeters and at the outermost limits, detectors for muons, the most penetrating particle to be detected. The whole device is often in a strong magnetic field so that momentum measurements may be made. An example of such a composite detector is shown in Fig.4.14.

This detector, called ZEUS, is positioned in a $e^- p$ collider at an accelerator lab DESY in Hamburg and is one used by the UCL particle physics group. The two beams are focused by quadruple lens (9) and then collide at the centre of the detector. The tracks of short-lived charged reaction products are recorded in the vertex chambers (3) and others in the drift chambers (4). The latter are surrounded by a magnetic field of 1.8 T and other magnets have to be introduced (6) to compensate for the effect on the beams themselves. The next layer is a calorimeter sandwich (1) of uranium (high stopping power) and scintillator (detector) where the energies of electrons and hadrons are measured. Further out, large-area wire chambers (5) detect the penetrating muons. Finally, a concrete wall (8) shields the surroundings from radiation.

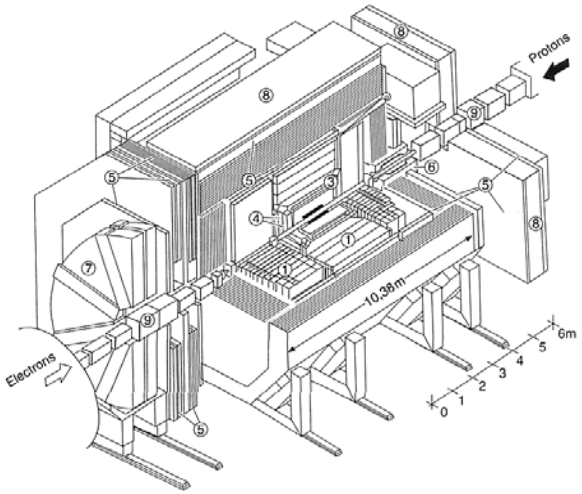

Fig.4.14 The ZEUS detector at the HERA collider at DESY, Hamburg